Nuclear Instruments and Methods in Physics Research A238 (1985) 307–314
North-Holland, Amsterdam

PERFORMANCE OF A LEAD–SCINTILLATOR SANDWICH HODOSCOPE WITH PHOTODIODE READOUT

G.-G. WINTER

Deutsches Elektronen-Synchrotron, DESY, Hamburg, Fed. Rep. Germany

J. AHME, J. MARKS, D. SCHÜTZ, H. SPITZER and H. WESTERMANN

II. Institut für Experimentalphysik, Universität Hamburg, Fed. Rep. Germany

H. GREIF and H. OBERLACK

Max-Planck-Institut für Physik und Astrophysik, Werner-Heisenberg-Institut für Physik, München, Fed. Rep. Germany

Received 4 February 1985

A matrix of nine lead–scintillator sandwich shower counters with wavelength shifter and photodiode readout was operated in an electron beam up to 6 GeV. The yield was measured to be 18500–25100 photoelectrons/GeV depending on the shape of the modules. An energy resolution of $\sigma/\sqrt{E} = 0.105$ was observed, the contribution from diode and amplifier noise being 29 MeV. The position resolution was determined as $\sigma \approx 3.0$ mm for 3 GeV electrons.

1. Introduction

Scintillator sandwich calorimeters with photomultiplier readout are a standard tool in high-energy physics experiments. They are limited in their application, however, by the complexity of the light collection and by their susceptibility to high magnetic fields. Recently the application of silicon photodiodes in combination with wavelength shifter (w.l.s.) readout has indicated a way to a system manageable even in high magnetic fields [1]. Low noise amplifiers matching the requirements of photodiodes were developed simultaneously. Large systems of scintillator calorimeters operating in high magnetic fields now seem feasible [2]. A system of moderate size is envisaged for the CELLO detector at PETRA. It may serve as a prototype for future larger installations.

2. Design of the calorimeter modules

We have tested an arrangement of nine prototype modules designed as electron tagging counters for the CELLO detector at PETRA. Since the counters will be mounted on a conical beam pipe, a cylindrical geometry was chosen. Fig. 1 shows the side and front view of the arrangement.

Each module consists of 45 samplings comprising 2.5 mm lead and 4 mm scintillator. The total length is $20.5 X_0$. The scintillators are separated from the lead by

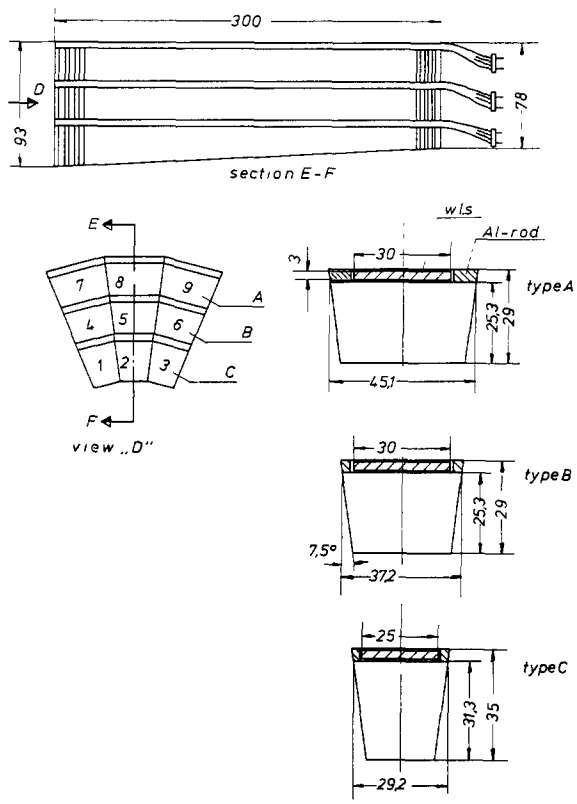

Fig. 1. Arrangement and dimensions of the nine calorimeter modules.

thin diffuse reflecting white foils. The light is collected from the broad side of the trapezoidally shaped scintillator sheets by one 3 mm thick w.l.s. bar leading to a silicon photodiode. The w.l.s. area matches the 1 cm^2 sensitive area of the photodiode used (Hamamatsu S1790). Two nylon threads with a diameter of 0.3 mm are used as spacers between the w.l.s. and the sandwich. The other three sides of the sandwich and the back of the w.l.s. are covered with white reflective foil. Finally the assembled module was inserted into a thin shrinking foil [3] which together with two aluminium rods provides enough stability for handling. The total thickness of reflecting and shrinking foils was < 100 μm. Owing to the cylindrical geometry the arrangement consists of three different types of modules. The height of the type C modules decreases with distance along its length, as to leave open a cone of 50 mrad. The transverse dimensions of the modules were chosen to be 2–3 effective radiation lengths thus allowing the use of side leakage into neighbouring modules in reconstructing the position of the shower.

For the scintillator–w.l.s. combination we have selected the polystyrene scintillator SCSN 38 with the specially matched shifter Y7 [4]. Of three different combinations tested this one gave the highest light yield. For testing we used a sandwich with dimensions $50 \times 50 \times 300$ mm^2 containing an average of 38 samplings of 2.5 mm lead. For light collection the w.l.s. was connected to a photodiode. The three scintillator types were available to us only in varying thicknesses (between 4 and 6 mm) at the time of the test. Table 1 shows the materials tested and the relative light yields from a 3 GeV electron shower normalized to a scintillator thickness of 4 mm. The normalization takes into account only the different amounts of energy deposition into the scintillator but not the dependence of the light transmission on the thickness of the sheets.

3. Electronics and experimental setup

The electronic signal of each photodiode was fed into a charge sensitive preamplifier and a shaping amplifier with a shaping time of 1.5 μs, developped at the MPI at Munich. The noise performance is 250 e_0 without load and in addition 4.7 [e_0/pF] for detector capacitance. The signal was digitized in a charge sensitive ADC of type LRS 2249 W *. All calorimeter modules were calibrated simultaneously by injecting a well defined amount of charge through test capacitors into the signal line.

The measurements were performed at DESY in a test beam with 1–6 GeV electrons. Four scintillator counters were used to define the position of the incident particle within a hole of radius of 2.5 mm. The momentum resolution of the beam was $\sigma_p/p \approx 1\%$. The angle of inclination of the ensemble of nine modules with respect to the beam axis was either 0 or 70 mrad, the latter corresponding to the average angle of incidence in the CELLO detector.

Table 1
Light yield for various scintillator–w.l.s. combinations

Scintillator	w.l.s.	Thickness (mm)	Relative light yield per 4 mm scintillator
Altustipe	BBQ	6	1.00
NE104B	BBQ	4	2.15
SCSN38	Y7	5	2.42

4. Light yield and intercalibration

For calibration an electron beam of 2, 3 and 5 GeV was centered on each module. Table 2 shows the results in equivalent photoelectrons (e_0) per GeV. We observe an average of 22200 e_0/GeV for type A modules, 25100 e_0/GeV for type B and 18530 e_0/GeV for type C. These yields have to be normalized to equal energy deposition. By means of a Monte Carlo (MC) simulation program [5] correction factors of 0.97, 1.0, 1.15 have been evaluated for type A, B, C, respectively. The remaining differences are due to the different light collection geometry for type A, B, C and fluctuations in the fabrication process. The normalized results are shown in the last column of table 2 as intercalibration constants relative to module 5. The absolute energy calibration constant is defined by the requirement that the sum over 9 modules equals the incoming energy.

In general we observe a striking improvement of the signal to noise ratio compared with our previously reported results [1]. This is due both to the better scintillator–w.l.s. combination and to a better light concentration. The small transverse dimensions of the modules allow a smaller shifter to cover a large solid angle of the module. In addition the trapezoidal shape favours efficient light collection. On a module with identical sampling, shifter and photodiode, but with a cross section of 50×50 mm^2 we measured a light yield of 14500 e_0/GeV. This clearly demonstrates the dependence of light yield on the module size.

As a check of our calibration we show in table 3 the average observed energy in each of the nine modules for a 5 GeV beam centered on module 5. Comparing this with a MC calculation we find in general agreement to within 10%.

* For matching reasons we have changed to the peak sensing ADC of type LRS 2259B in a consecutive test with 36 modules, not reported here.

Table 2
Yield and intercalibration constants of the nine modules

Module	Type	Yield [e_0/GeV]	Average [e_0/GeV]	Corrected yield [e_0/GeV]	Intercalibration constant
1	C	18100	18530	20800	0.87
2		19500		22400	0.94
3		18000		20700	0.87
4	B	24500	25100	24500	1.03
5		23800		23800	1.00
6		27000		27000	1.17
7	A	19600	22200	19100	0.81
8		23500		22900	0.96
9		23600		23000	0.96

Table 3
Average energy (in MeV) deposited in each of the nine modules when a 5 GeV electron beam hits the center of the module 5. The numbers in brackets are from a Monte Carlo simulation.

71.4	260.3	62.0
(64.8)	(232.6)	(63.7)
module 1	module 2	module 3
143.6	4133.6	117.2
(144.9)	(4069.7)	(144.1)
module 4	module 5	module 6
60.0	148.5	61.6
(59.5)	(171.2)	(59.8)
module 7	module 8	module 9

5. Linearity and energy resolution

Fig. 2 shows the measured energy distributions in module 5 for incoming electrons of 1–6 GeV hitting the center of the module. The mean energy and the energy resolution were evaluated by gaussian fits to these distributions. The mean of the measured energy is shown in fig. 3. Also shown in this figure are the values of the mean of the energy summed over 5 modules (#2, 4, 5, 6, 8) and over all 9 modules. Clearly the measured energy varies linearly with the incoming energy for the three summations. The same is true for electrons at 70 mrad incidence. The energy distributions contain a high energy tail of typically 1% which is due

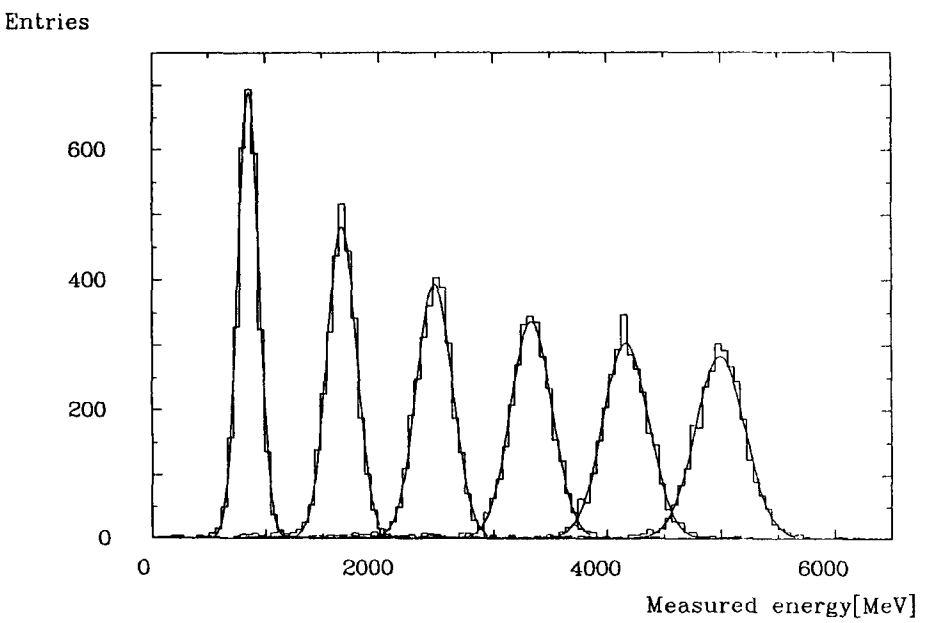

Fig. 2. Measured energy distributions in module 5 for incoming electrons of 1–6 GeV hitting the center of the module.

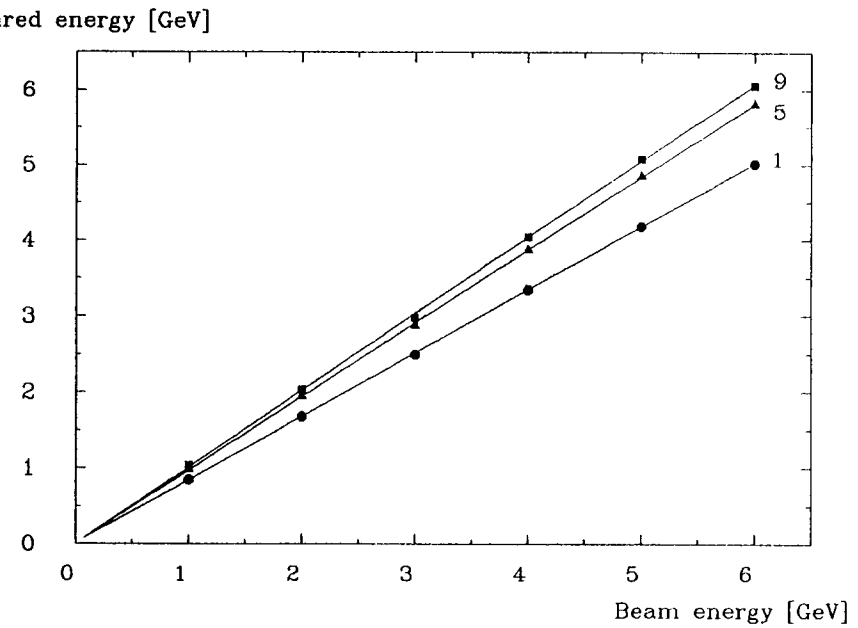

Fig. 3. Mean of the measured energy vs the beam energy for 1 module and for the sum of five and nine modules.

to the nuclear counter effect of rear leakage particles hitting the photodiode.

The energy resolution as shown in fig. 4 levels down to about $11\%/\sqrt{E}$ at high energies and shows an excess above an $1/\sqrt{E}$ behaviour at small energies. This excess increases with the number of modules used for summation, and is due to diode and amplifier noise. We have fitted the expression

$$\sigma/\sqrt{E} = \sqrt{a^2 + b^2\,E + \sigma_D^2/E}$$

to the data. The results of the fits are given in table 4. Here $a^2 = \sigma^2_{\text{sampling}} + \sigma^2_{\text{leakage}}$ contains the sampling and side leakage fluctuations, $b = 0.01$ (fixed) is the contribution from the spread of the beam energy and σ_D is the contribution from diode and amplifier noise. Leakage through the rear of the module ($< 1\%$) has been neglected. We find an average of $\sigma_D = 29$ MeV per module. This is in good agreement with the directly measured noise of 800 e_0 and the average light yield of ≈ 22000 e_0/GeV for an individual module. The energy resolution for a 70 mrad beam shows a similar behaviour.

Table 4
Parameters from a fit of $\sigma/\sqrt{E} = \sqrt{a^2 + b^2E + \sigma_D^2/E}$ to the data. The values a_{MC} result from the MC calculation.

	mrad incidence	$a(\sqrt{GeV})$	σ_D(MeV)	a_{MC}
single module	0	0.105	29	0.105
Σ(5)	0	0.100	67	0.096
Σ(9)	0	0.098	98	0.093
Σ(2)	70	0.103	30	
Σ(3)	70	0.103	52	
Σ(9)	70	0.095	106	

To investigate the dependence of the measured energy and the energy resolution on the beam position we have made a scan from the center of module 2 to the center of module 8 along the center line of the setup. The beam energy was 3 GeV. The response of modules 2, 5 and 8 together with the sum over nine modules is shown in fig. 5a for 0 mrad beam incidence. The sum response is uniform within $\pm 4\%$, except for the position of the w.l.s. and a region of about 10 mm from the edges.

A similar scan was performed with a beam of 3 GeV incident at 70 mrad. As shown in fig. 5b a similar uniformity is obtained, and the drop of the response at the shifter position is washed out. We observe an energy resolution (fig. 6) of 12–14% in the central region (10 mm off the edges) except near the w.l.s. positions where it rises to 17%.

6. Position resolution

We have used the data from this scan to investigate the position resolution. A simple method for determining the position of an incoming particle is to calculate the center of gravity (x_c) of the energy deposition:

$$x_c = \frac{\Sigma_i x_i E_i}{\Sigma_i E_i} \quad (i = 2, 4, 8),$$

where x_i is the coordinate of the center of the i^{th} module and E_i is the energy deposited in it. In fig. 7 we show the calculated position x_c versus the position of the beam for 70 mrad incidence. The bars indicate the r.m.s. widths of the x_c distributions determined individually for the upper and lower parts. x_c does not vary linearly with the beam position (x): At the center of a module a slow variation occurs, whereas at the border a strong variation is observed. This behaviour is expected and has been discussed in the literature for 0^0 incidence [6]. For 70 mrad incidence a MC simulation reproduces well the observed dependence of the center of gravity on the position of the beam as demonstrated by the solid curve in fig. 7.

We have parametrized the relationship between x_c and the true position x_t and used it to calculate x_t. In fig. 8a the distribution of $\Delta x = x_t - x$ averaged over the scan region is shown. The central part of this distribu-

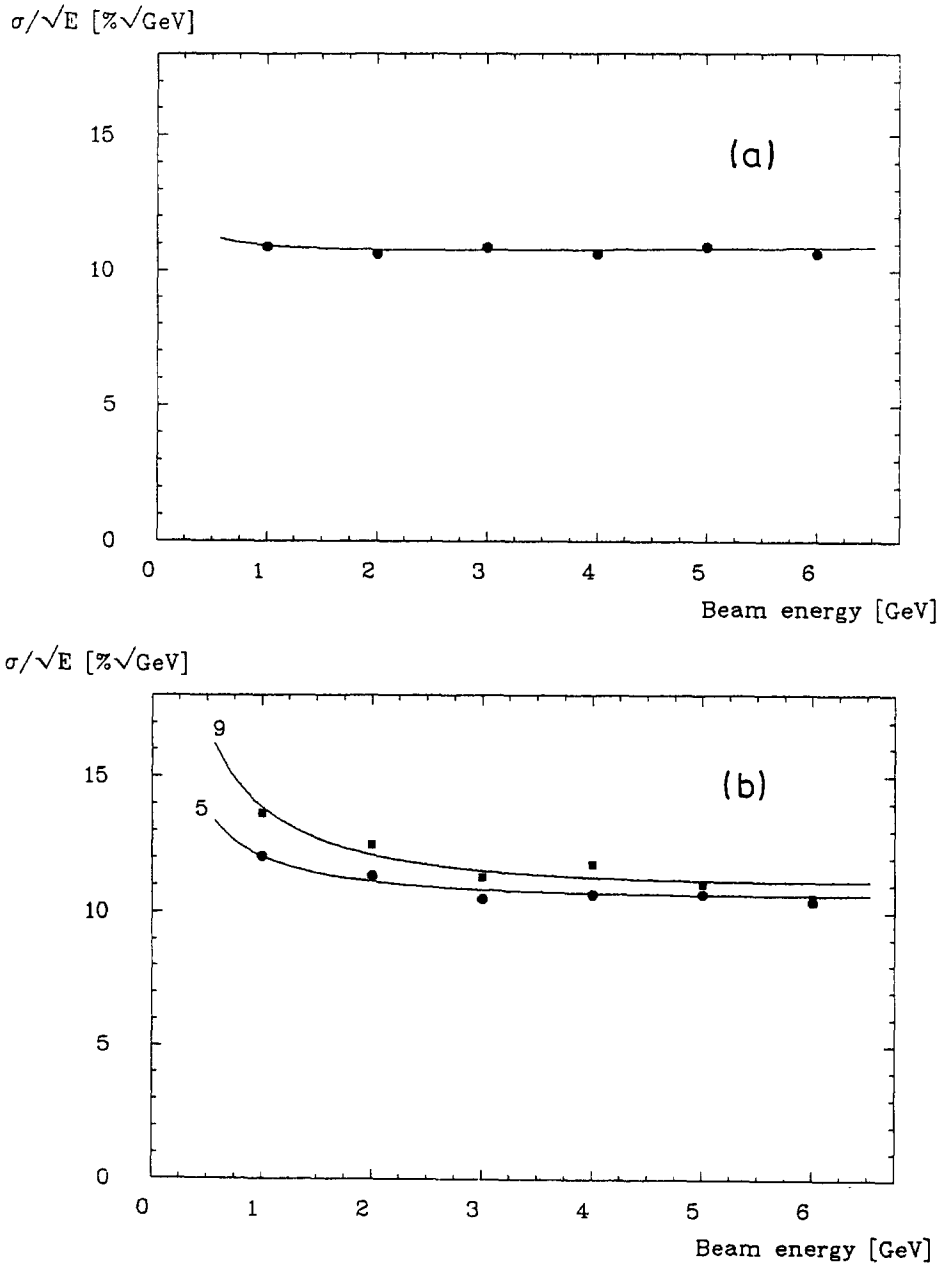

Fig. 4. Energy resolution for a single module (a) and for the sum over five and nine modules (b).

tion is Gaussian (solid line) with a width of 3.5 mm. This includes a small contribution from the incoming beam spot of 2.5 mm radius.

We have also investigated the position resolution between two modules not separated by a shifter in a scan from the center of module 4 to the center of module 6. Here the Δx distribution as shown in fig. 8b has a width of 2.5 mm.

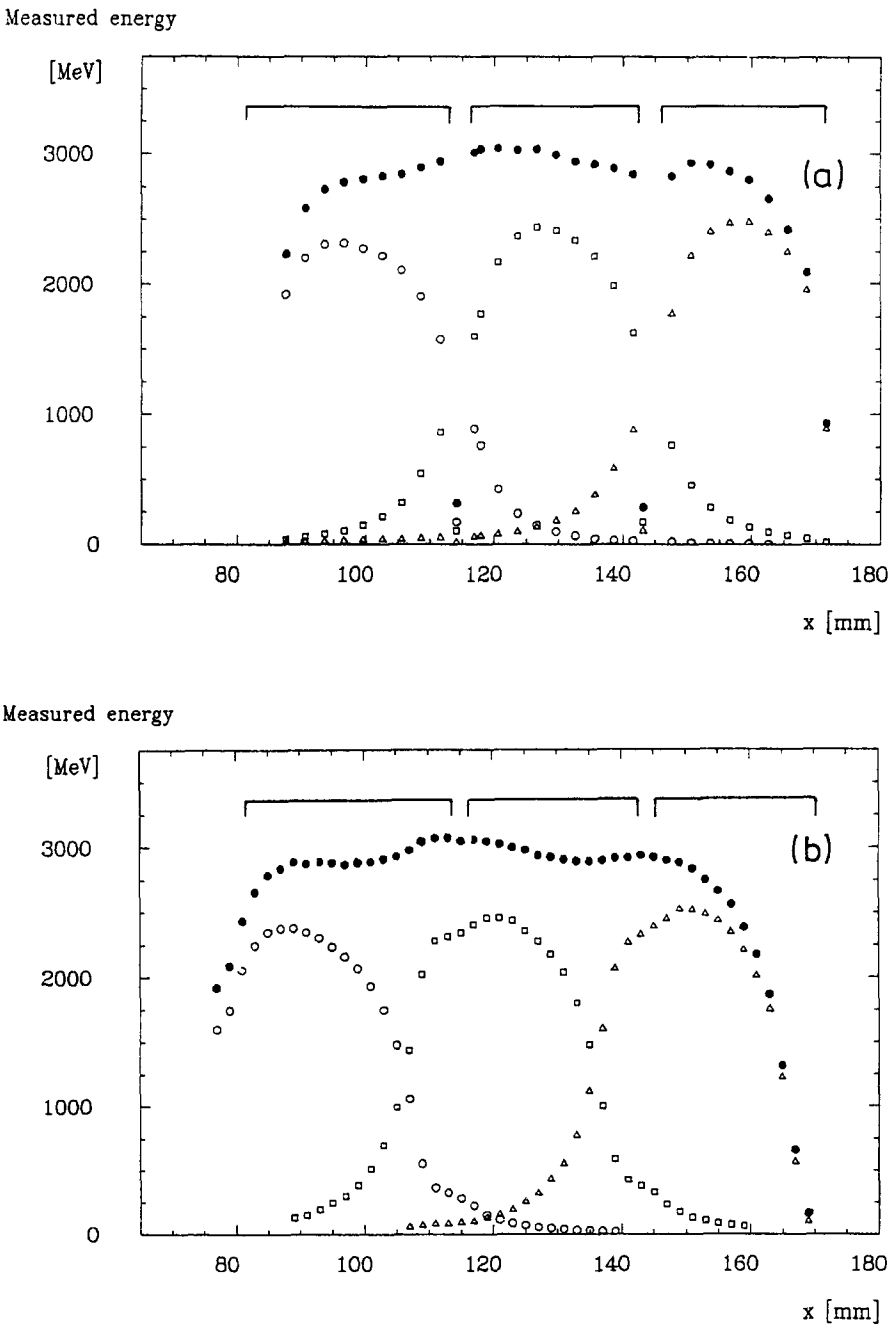

Fig. 5. Energy vs vertical position (x) of beam incidence. Shown is the individual response of the modules along the scanning line and the sum over all nine modules. The positions of modules and shifters are indicated at the top. (a) For a 0^0 incident beam, (b) for a 70 mrad incident beam. Note the shift of response with respect to the module positions. This is due to the shower development along the 70 mrad direction.

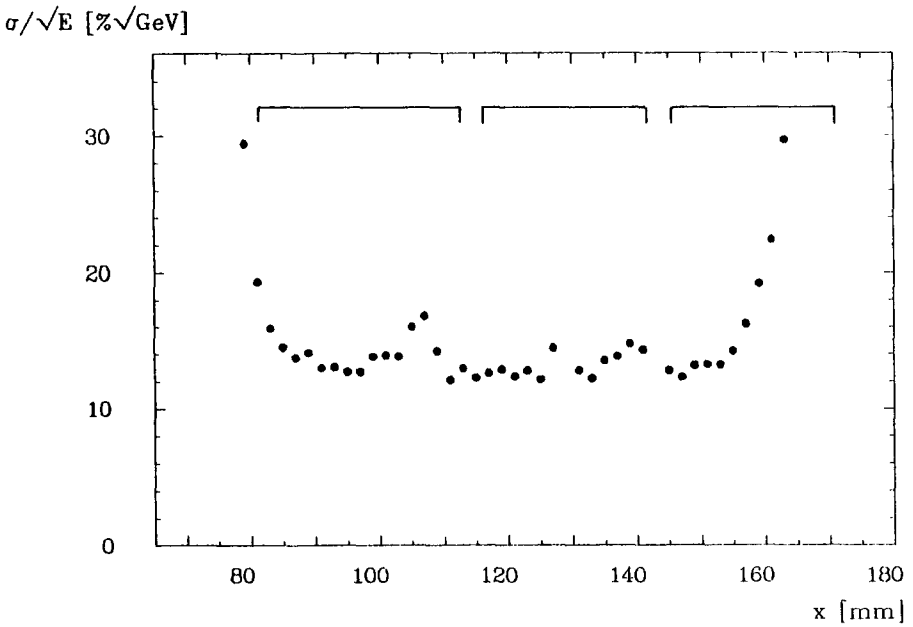

Fig. 6. Energy resolution vs vertical position (x) for the sum of all nine modules. The beam energy is 3 GeV, beam incidence 70 mrad. The positions of modules and shifters are indicated at the top.

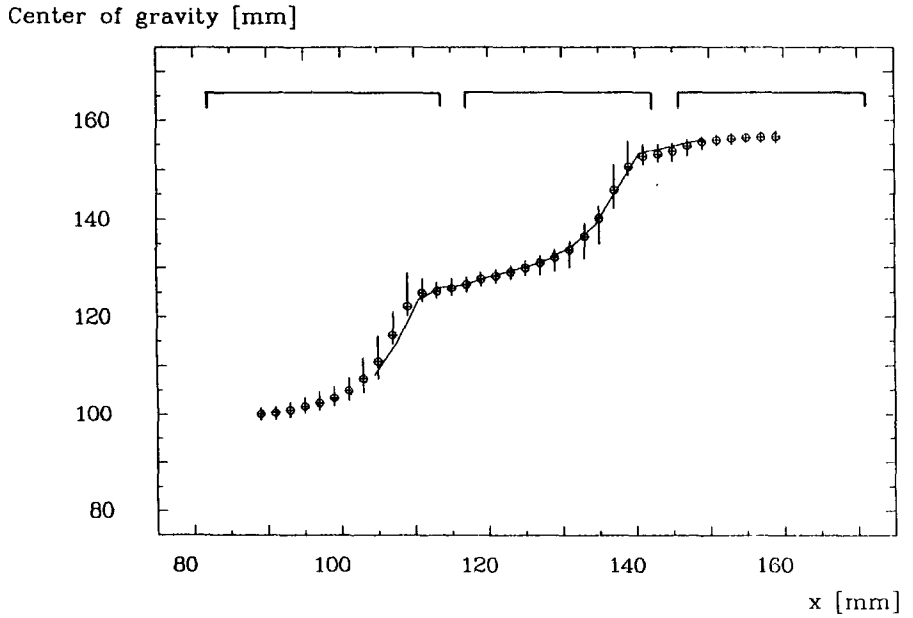

Fig. 7. Center of gravity vs beam position (x) for the vertical scan. Beam incidence is 70 mrad. The full line is from a MC simulation. The positions of modules and shifters are indicated at the top.

7. Summary

A prototype system for a small angle tagging calorimeter for CELLO at PETRA has been tested in an electron beam of 1–6 GeV. It consists of lead–scintillator sandwiches, the light being collected via w.l.s. bars onto silicon photodiodes. A light yield of 18500–25100 e_0/GeV was observed depending on the shape of the modules. The resulting energy resolution was found to be $\sigma/\sqrt{E} \approx 0.11$ with a noise contribution of 29 MeV per module. The spatial resolution was determined from the energies deposited in adjacent modules, it averages 3 mm depending on the location in the module. With such improvements in light yield and signal/noise ratio

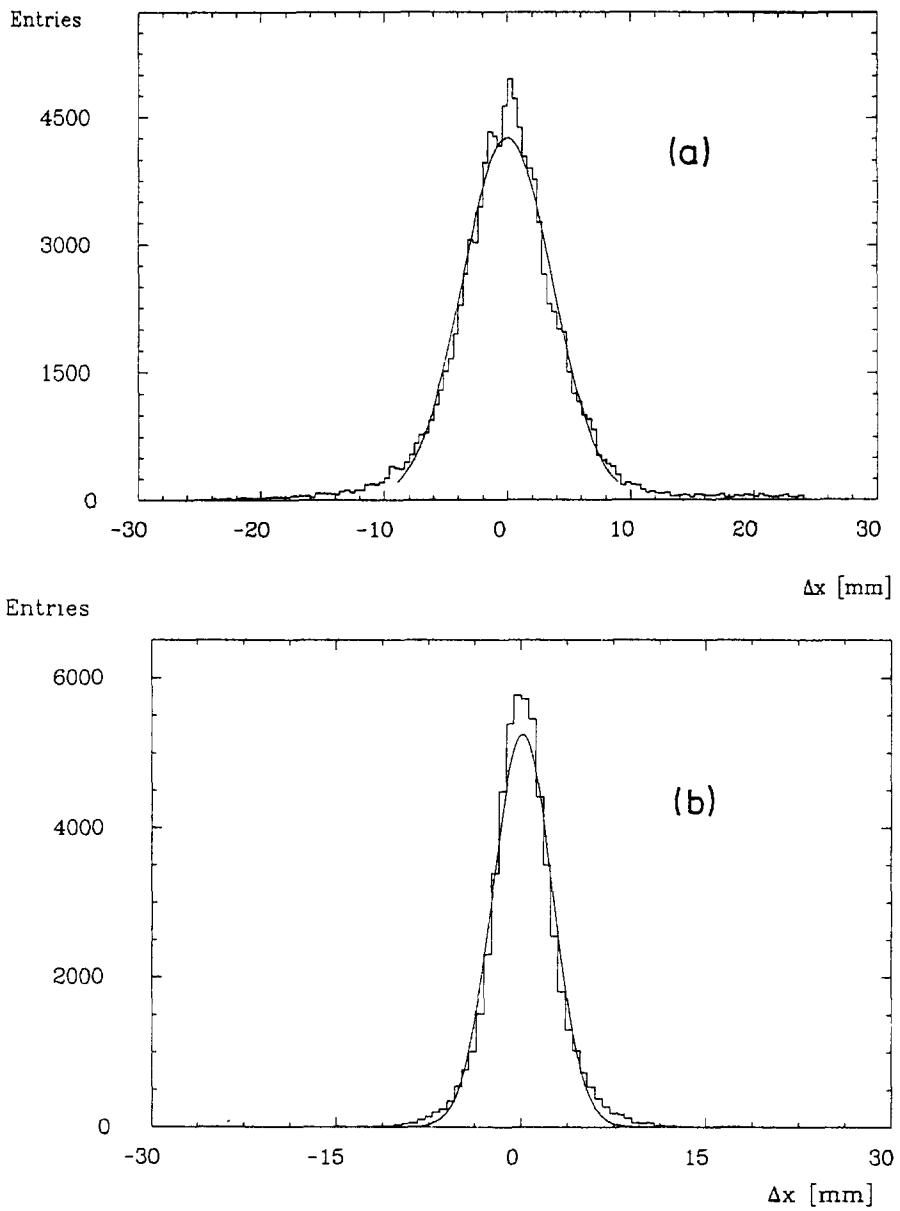

Fig. 8. Position resolution Δx (calculated position minus beam position) (a) for the vertical scan, (b) for the horizontal scan.

achieved with the photodiode readout energy resolutions comparable to a photomultiplier readout can be obtained for energies above a few hundred MeV.

We thank P. Weissbach and his group at the MPI in Munich for the support in the development of the electronics. We are indebted to Dr. P. Bussey for comments on the text. This work was partly supported by the Bundesministerium für Forschung und Technologie (BMFT).

References

[1] J. Ahme et al., Nucl. Instr. and Meth. 221 (1984) 543.
[2] H. Dietl et al., Topical Seminar on Perspectives for experiments at future high energy machines, San Miniato, Italy (1984).
[3] NALOPHAN foil from KALLE, Wiesbaden.
[4] T. Kamon et al., Nucl. Instr. and Meth. 213 (1983) 261.
[5] R.L. Ford and W.R. Nelson, EGS Code, SLAC Rep. 210 (1978).
[6] G.A. Akopdjanov et al., Nucl Instr. and Meth. 140 (1977) 441.